J Solid State Electrochem (2010) 14:1481–1486
DOI 10.1007/s10008-009-0976-1

ORIGINAL PAPER

Synthesis of different polymorphic modifications of calcium oxalate by electrodeposition

Sumy Joseph · P. Vishnu Kamath

Received: 4 August 2009 / Revised: 7 November 2009 / Accepted: 10 November 2009 / Published online: 9 December 2009

Abstract Different hydrates of calcium oxalate have been electrodeposited by electrogeneration of acid at the anode from an EDTA-stabilized calcium nitrate bath containing dissolved oxalate ions. The deposition is controlled by varying the bath pH, temperature, and current density. Formation of metastable $CaC_2O_4{\cdot}2H_2O$ is favored at high current densities at ambient temperature, whereas the thermodynamically stable $CaC_2O_4{\cdot}H_2O$ is formed at elevated bath temperatures. Both the polymorphs show oriented growth with respect to the substrate normal under different deposition conditions.

Keywords X-ray diffraction · Electrochemical growth · Polycrystalline deposition · Calcium compounds

Introduction

Calcium oxalate is a major component of kidney stone and crystallizes in three different polymorphic modifications [1]. The deposition of calcium oxalate has generated much interest, as it is a model system to investigate the crystallization process and the effect of crystallization conditions on polymorph selection. It is also a good system to study hydrate-phase transformations. Among the three calcium oxalate hydrates, the monohydrate is the thermodynamically stable phase under ambient conditions. Metastable phases with higher solubility are obtained when there is a departure from equilibrium such as a high degree of supersaturation. Therefore, there is much interest in studying the conditions under which the calcium oxalate monohydrate (COM) crystallization is prevented and dihyhrate (COD) is favored [2]. The additive mediated preferential growth of COD has been studied using natural as well as synthetic molecules. These molecules includes sodium di-isooctyl sulfosuccinate [3], poly(ethyleneglycol)-*block*-poly(methacrylicacid) [4], polypeptides [2], synthetic biopolymers and proteins [5]. The role of additives has also been investigated for the growth of calcium oxalate with different morphologies.

Synthesis of calcium oxalate in the presence of surfactants is also investigated [6]. Ionic surfactants inhibit the growth and aggregation of COM and promote the crystallization of COD. Nonionic surfactants also stimulate the growth of COD. Polymers with carboxylate moieties separated by a distance shorter than 2.52 Å had a better inhibitory effect on the crystallization of the monohydrate compared to others in which they are separated by a larger distance [4]. According to Gardner [7], the metastable calcium oxalate trihydrate (COT) is converted into the thermodynamically stable COM even in the solid state. But based on the investigations of Brecelvi and Startic [8], the transformation is solution-mediated. Davis modification of the Debye–Huckel equation [9] suggests that the solubility products of the different hydrates vary in the order COM< COD<COT. But the measured solubility products are very close to each other and the initial product of chemical synthesis is always a mixture of all the hydrates. Eventually, the mixture gets transformed into the stable COM. COM crystallizes in the monoclinic crystal system, whereas COD crystallizes with tetragonal symmetry, and COT with triclinic symmetry.

Electronic supplementary material The online version of this article (doi:10.1007/s10008-009-0976-1) contains supplementary material, which is available to authorized users.

S. Joseph · P. V. Kamath (✉)
Department of Chemistry, Central College, Bangalore University, Bangalore 560 001, India
e-mail: vishnukamath8@hotmail.com

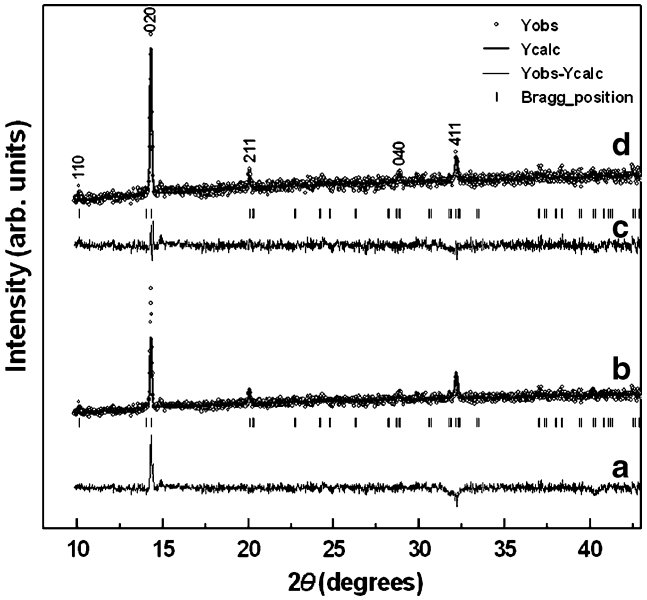

Fig. 1 Rietveld fit of PXRD profile of a $CaC_2O_4{\cdot}2H_2O$ coating obtained from an EDTA-stabilized bath at pH 9: (**a**) and (**b**) are, respectively, the difference profile and calculated pattern obtained without incorporating orientation, (**c**) and (**d**) are the difference profile and the calculated pattern obtained by incorporating 020 orientation laid over the observed pattern

The crystallization of the same material in different crystal structures with variation in the solvent content results in the formation of solvates. When the solvent of crystallization is water, the phases are named as hydrates. Conventionally, this type of polymorphism is known as pseudopolymorphism. The usage of the term 'pseudopolymorph' for hydrates/solvates is a subject of recent discussion [10–12].

We have for some time been interested in the use of electrochemistry to affect the crystallization of a variety of solids from suitable precursor solutions [13]. While electrodeposition (using single-crystalline and polycrystalline substrates) can be used to direct oriented crystallization [14] and engineer crystal morphology [15], there are few instances of the study of polymorphism by electrochemistry. $CaCO_3$ exhibits extensive polymorphism. Calcite is the thermodynamically stable phase, whereas vaterite and aragonite are metastable. The aragonite modification could be electrodeposited in the presence of Mg^{2+} [16]. It is unclear if the polymorphism is induced by the deposition conditions or by the presence of Mg^{2+} ions.

Given the existence of various crystalline hydrates of calcium oxalate, this is a model system for the exploration of electrochemistry-induced polymorph selection. Windhausen and Switzer [17] deposited calcium oxalate by the cathodic reduction of an acidic bath containing Ca^{2+} and $C_2O_4^{2-}$ ions. Calcium oxalate precipitates at pH 5 and above. On passing current, a steep increase in the pH is observed close to the cathode due to hydrogen evolution and other companion reactions. Prof. Switzer refers to this phenomenon as 'electrogeneration of base' [18]. COM deposits on the cathode [17]. COT was also deposited at high degrees of supersaturation brought about by enhancing the bath concentration [19, 20].

In this paper, we study how the electrodeposition parameters affect phase selection among the hydrates of calcium oxalate.

Experimental section

Synthesis

Electrodeposition was carried out using an EG&G (PARC) Versastat IIA scanning potentiostat driven by Power Suite software (current density 1–6 mA cm^{-2}, t 15–60 min., T 25-60 °C). Calcium oxalate coatings were obtained at the

Table 1 Refined parameters obtained by the Rietveld fit of the observed PXRD profiles of calcium oxalate

Space group		Fig. 1 COD $I4/m$	Fig. 2 COD $I4/m$	Fig. 5 COM $P2_1/c$	Fig. 6 COM $P2_1/c$
Cell parameters	a (Å)	12.385(1)	12.386(3)	6.234(6)	6.244(3)
	b (Å)	12.385(1)	12.386(3)	14.598(1)	14.599(2)
	c (Å)	7.356(4)	7.354(2)	9.997(5)	9.930(1)
	β (deg)	90	90	107.14(5)	107.27(2)
Profile parameters	U	0.469	0.223	1.268	0.923
	V	−0.0867	−0.125	−0.5426	−0.0965
	W	0.0142	0.0335	0.0648	0.0225
	η	0.164	0.445	0.1979	0.213
	X	0.0233	−0.0035	0.0491	0.0218
Goodness-of-fit parameters	R_{Bragg}	0.27	0.26	0.32	0.31
	R_f	0.24	0.27	0.27	0.24
	χ^2	1.14	1.5	1.15	1.3

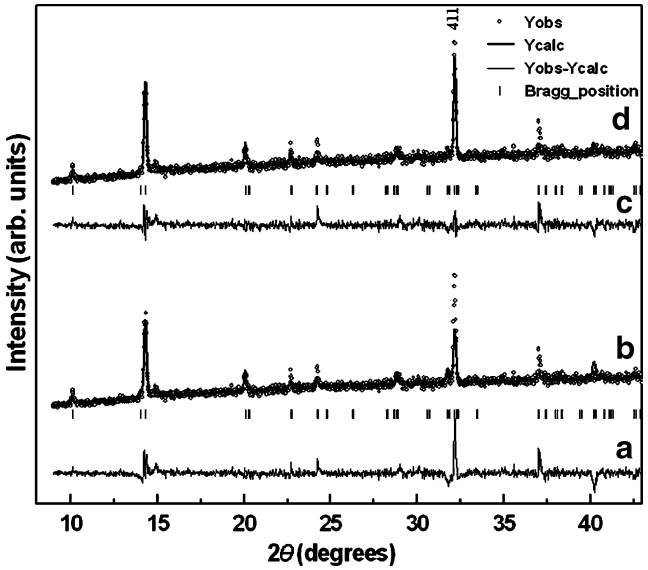

Fig. 2 Rietveld fit of PXRD profile of a thick $CaC_2O_4{\cdot}2H_2O$ coating obtained from a EDTA-stabilized bath at pH 11: **a** and **b** are, respectively, the difference profile and calculated pattern obtained without incorporating orientation, **c** and **d** are the difference profile and calculated pattern obtained by incorporating 411 orientation, laid over the observed pattern

anode. $Ca(NO_3)_2$ and disodium salt of oxalic acid were purchased from Aldrich Chemical Co. (USA) and used as such. EDTA was obtained from Lancaster (UK) and used as such. All solutions were prepared using ion-exchanged Type-I water (Milli Q Academic Water Purification System, specific resistance 18.3 MΩ cm).

In a typical synthetic procedure, the bath was prepared by mixing equal volumes of $Ca(NO_3)_2$ (0.05 M) and EDTA (0.075 M) solutions. The pH of the bath was then raised to a predetermined value in the range 6–11.5 by adding 4 M NaOH solution. To this stabilized bath, an equal volume of sodium oxalate was added (0.05 M). A polycrystalline stainless steel flag (SS 304, surface area 4.5 cm^2) was used as a working electrode and polarized anodically with respect to a saturated calomel electrode (SCE). A Pt flag (surface area 8 cm^2) was used as the counter electrode. Prior to electrodeposition, all the electrodes were cleaned with detergent and electrochemically polished by polarizing them anodically, cathodically, and again anodically in 1 M KOH and then anodically in 1 M HCl. Each step was for a duration of 30 s.

Characterization

All the coatings were studied by powder X-ray diffraction (PXRD) by mounting the electrode directly on a Bruker aXS Model D8 Advance powder diffractometer, operated in reflection geometry (Cu Kα radiation, λ=1.541 Å). Data were collected at a continuous scan rate of 1°2θ per minute and then rebinned into 2θ steps of 0.02°.

The Rietveld technique was used for structure refinement (FULLPROF .2 k code, version 3.3 June 2005-LLB JRC). All PXRD profiles were fit using the published structures of $CaC_2O_4{\cdot}H_2O$ (ICSD CC 45115) and $CaC_2O_4{\cdot}2H_2O$ (ICSD CC 30783). In all the refinements, the pseudo-Voigt line shape function with five variables (U, V, W, X, and η) is used to fit the experimental profiles. The background adjustment in the calculated patterns was made using a six-coefficient or a 12-coefficient polynomial function. The scale factor, zero-shift, profile parameters, cell parameters, and atom position parameters were refined sequentially in this order. Finally, all the parameters were refined together.

In some of the patterns, the observed intensity of certain select Bragg reflections was found to be higher than that expected from the crystal structure data. Residual intensity is seen in the difference profile obtained at the end of the structure refinement procedure at Bragg angles corresponding to these reflections. This anomalous increase in intensity is on account of oriented crystallization [21]. In such instances, the Rietveld refinements were repeated by incorporating preferred orientation parameters G_1 and G_2 in the modified March's Function. $0<G_1<1$ corresponds to a crystal with a platy habit. G_2=0 corresponds to a fully oriented coating and G_2=1 to a coating without any preferred orientation.

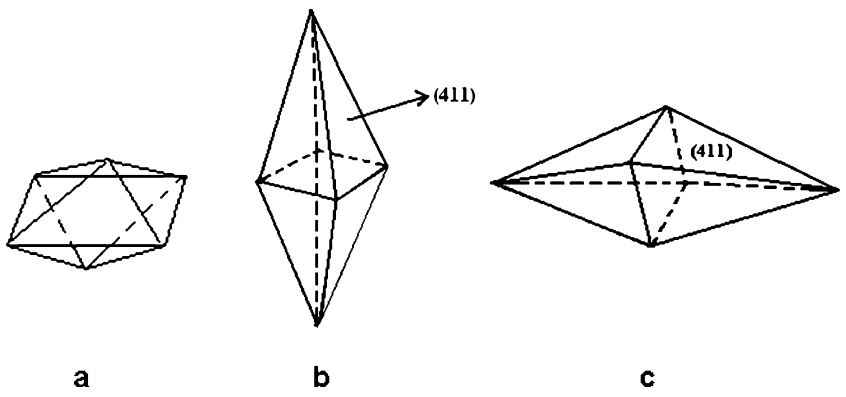

Fig. 3 Schematic drawings of a polyhedron bound by {411} planes viewed perpendicular to the crystallographic axes

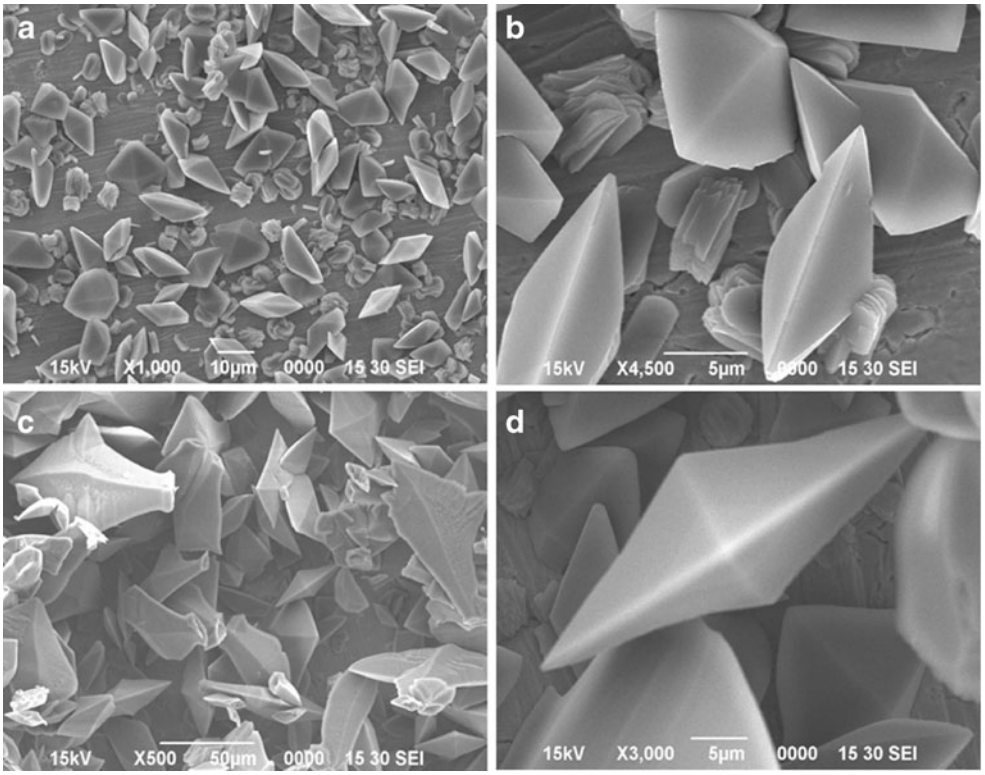

Fig. 4 Scanning electron micrographs of $CaC_2O_4{\cdot}2H_2O$ coatings deposited at 6 mA/cm^2. **a**, **b** Bath pH 9.0 and **c**, **d** 11.0

Scanning electron micrographs were obtained using JEOL JSM 6490 LV microscope by mounting a small piece of the coated electrode on conducting carbon tape and sputter coating with Pt to improve the conductivity.

Results and discussion

Earlier work [17, 19, 20] on the electrodeposition of calcium oxalate was done by cathodic reduction of acidic aqueous solutions containing Ca^{2+} and $C_2O_4^{2-}$ ions. In this study, we use an alternative electrosynthetic method for the deposition of calcium oxalate. EDTA is used to complex the Ca^{2+} ions. Ca–EDTA complex has a high stability constant (pK=10.59 at pH 7), whereby calcium oxalate precipitation is suppressed in the entire pH range of 5–13. The use of a complexing agent provides a method by which the free [Ca^{2+}] in the bath can be finely tuned by varying the [EDTA]/[Ca^{2+}] ratio. Calcium oxalate deposition is induced by bringing down the pH. Acidic pH is generated at the anode on account of oxygen evolution—a phenomenon described as 'electrogeneration of acid' [22]. The stability constant of Ca–EDTA complex decreases as the pH is lowered, leading to the release of free Ca^{2+} ions by acid hydrolysis of the complex. The Ca^{2+} ions precipitate calcium oxalate.

As the pH changes take place close to the anode, the calcium oxalate is deposited on the anode in the form of a coating. The deposition of a white coating is visually seen on the anode after a few minutes of deposition. The PXRD pattern of the deposited coating (deposition current 3 mA cm^{-2}; time 30 min.; pH 6) shows the phase to be COD (a=12.371 Å; b=12.371 Å; c=7.357 Å). The nature of the deposit remains unchanged in the pH window 6 to 9.

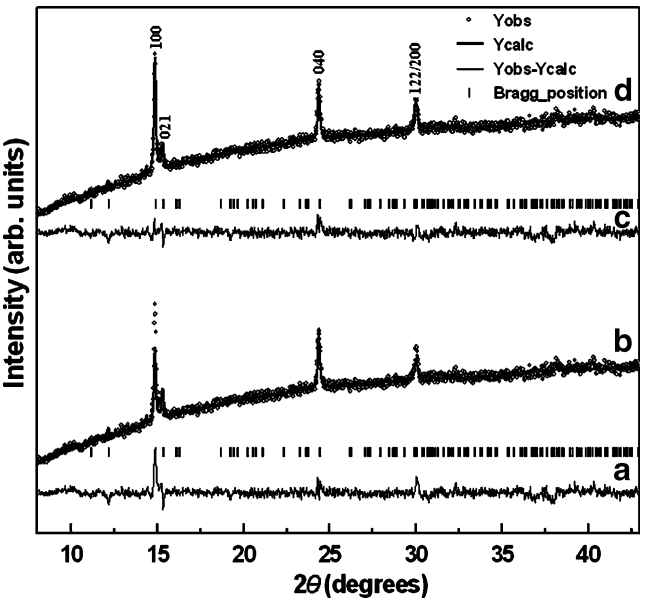

Fig. 5 Rietveld fit of PXRD profile of a $CaC_2O_4{\cdot}H_2O$ coating obtained from a EDTA-stabilized bath at 6 mA/cm^2, pH 11.0, T=60 °C: **a** and **b** are, respectively, the difference profile and calculated pattern without incorporating orientation, **c** and **d** are the difference profile and calculated pattern obtained by incorporating 100 orientation laid over the observed pattern

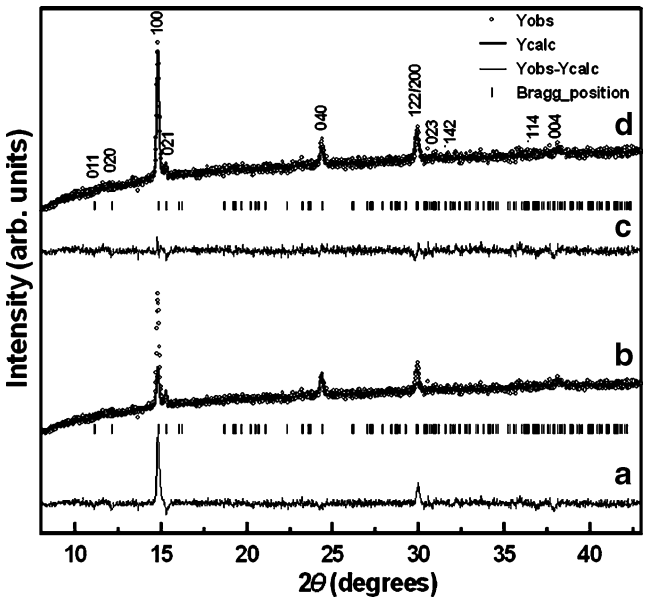

Fig. 6 Rietveld fit of PXRD profile of a $CaC_2O_4{\cdot}H_2O$ coating obtained from a EDTA-stabilized bath at 3 mA/cm^2, pH 11.0, T=60 °C: **a** and **b** are, respectively, the difference profile and calculated pattern obtained without incorporating orientation, **c** and **d** are the difference profile and calculated pattern obtained by incorporating 100 orientation laid over the observed pattern

A Rietveld fit of the observed profile (Fig. 1a, b) shows that the relative intensity of the 020 reflection in the observed pattern is much higher than the calculated value. This excess intensity manifests itself in the difference profile (Fig. 1a) at the Bragg position of the 020 reflection. Such anomalous variation in the intensities is generally due to oriented crystallization [21]. On repeating the refinement by incorporating preferred orientation parameters along the *b*-crystallographic axis, a good match of the calculated and observed diffraction profile is realized (Fig. 1c,d) (G_1= 0.368; G_2=0.853). All coatings obtained in the pH range 6–9 are found to have a *b*-axis orientation. The refinement results along with goodness-of-fit parameters are given in Table 1. The goodness-of-fit parameters are higher than those obtained in typical refinement studies which employ bulk powder samples. However, more important than the *R* values is the nature of the difference profile [23] which is seen to be smooth and featureless after the inclusion of the preferred orientation parameters.

Above pH 9, a dramatic enhancement in the intensity of the 411 reflection from 14% to 75% relative to the 020 reflection is observed (Fig. 2). A Rietveld fit yields refined values of the orientation parameters, G_1=0.56 and G_2=0, indicating a fully oriented coating. As the pH increases, the stability of the complex also increases, leaving behind a lower concentration of the free [Ca^{2+}] slowing down the rate of deposition.

The crystallites have a bipyramidal morphology. The anomalous enhancement in the intensity of the 411 reflection suggests that the triangular faces of the bipyramidal crystallites comprise {411} planes (see schematic in Fig. 3). The base of the bipyramids is a rhombus, in the *a*–*b* plane. The short axis of the bipyramids is parallel to the *c*-crystallographic axis and the long axis is parallel to the *b*-

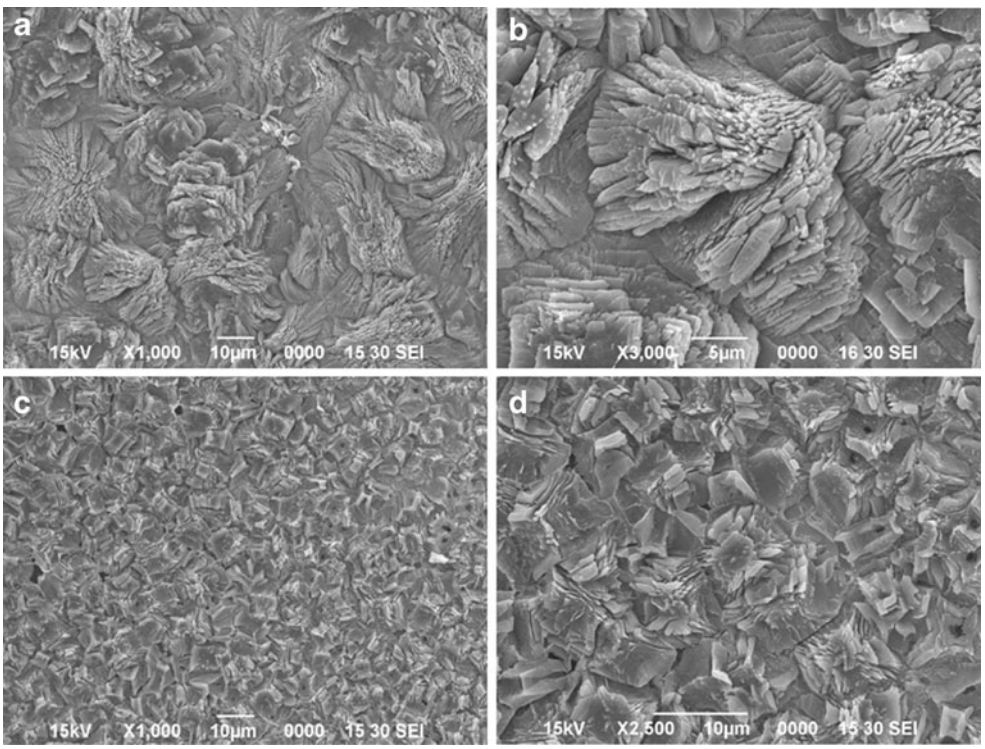

Fig. 7 Scanning electron micrographs of $CaC_2O_4{\cdot}H_2O$ coatings deposited from EDTA-stabilized bath at **a**, **b** 3 mA cm^{-2} and **c**, **d** 6 mA cm^{-2} at 65 °C, pH=11.0

crystallographic axis. This morphology is a result of the slower growth of crystallites along [001] compared to the *a*–*b* plane. Irrespective of the planes that comprise the crystallite macrostructure, the tilt angle of the crystallites with respect to the substrate determines the out-of-plane orientation. The *b*-axis orientation arises when the long axis of the crystallites is normal to the substrate. The morphology shown in Fig. 3 is observed in the SEM images (Fig. 4). Although the PXRD shows the presence of a single-phase COD, the SEM images show a small volume fraction of crystallites comprising stacking of platelets of COM.

Deposition at a low-current density (1 mA cm^{-2}) at the ambient temperature resulted in the formation of a mixture of COM and COD (see Supporting Information SI.1 for the PXRD pattern). At a lower current density, the deposition rate of the coating is much slower compared to that at higher current density. This leads to the solution-mediated transformation of the initially formed calcium oxalate dihydrate to calcium oxalate monohydrate. The SEM micrographs of the above sample clearly indicate the presence of both phases (Supporting Information SI.2). There are two kinds of morphologies, a granular base coat and highly crystalline particles several microns in length that could be seen at a lower magnification itself. The particle size of the granules is in the region of 10 μm. At a higher magnification, each of the granular particles is seen to be a collection of highly crystalline needles radiating out from a common interior origin. The question arises: is the COM directly deposited from solution or is it a product of the transformation of the initially deposited COD? The answer is not clear from our experiments. However, Ostwald's law [24] predicts that the thermodynamically least stable phase is the first to form during crystallization from a solution or melt. Based on this general understanding, we hypothesize that COD, the less-stable phase is formed first. COD then transforms to COM. Ostwald's law envisages a solution-mediated dissolution–reprecipitation mechanism for such transformations. Our surmise is based on the fact that the two phases co-exist in the same coating.

When the deposition was carried out at a higher temperature (60 °C), the thermodynamically stable COM was electrodeposited (pH 11.0, current density 6 mA cm^{-2}). COM crystallizes with monoclinic symmetry (space group $P2_1/c$, a=6.24 Å, b=14.58 Å, c=9.89 Å, β=98.9º). A Rietveld fit of the observed profile showed a mild 100 orientation of the crystallites (G_1=0.70; G_2=0.71; Fig. 5).

At a higher temperature, the excess thermal energy facilitated the complete transformation of the metastable COD to the thermodynamically stable COM. When the rate of deposition is decreased by decreasing the current density to 3 mA cm^{-2}, a highly oriented COM coating was observed (G_1=0.61; G_2=0.49; Fig. 6). The degree of orientation increases at a lower current density. The SEM images of COM coatings (Fig. 7) look entirely different from that of the dihydrate. The coating is continuous. The individual crystallites comprise platelets originating from a nucleus and radiating outside. Coating that is strongly oriented along the 100 direction has a similar morphology compared to that of the less-oriented coating.

Conclusions

In conclusion, we demonstrate in this paper one of the few applications of electrochemistry in the synthesis of polymorphs. Different polymorphic modifications of calcium oxalate have been deposited by variation in deposition conditions. Although the deposited phases are hydrates of calcium oxalate, there is further scope for investigating the polymorph selection in other systems.

Acknowledgments The authors thank the University Grants Commission, Government of India (GOI) for financial support. SJ and PVK thank the Department of Science and Technology, GOI for the award of a Junior Research Fellowship and Ramanna Fellowship, respectively.

References

1. Tomažić B, Nancollas GH (1979) J Cryst Growth 46:355
2. Wesson JA, Worcester E (1996) Scanning Microsc 10:415
3. Tunik L, Furedi-Milhofer H, Garti N (1998) Langmuir 14:3351
4. Zhang DB, Qi LM, Ma JM, Cheng HM (2002) Chem Mater 14:2450
5. Jung T, Kim WS, Choi CK (2005) J Cryst Growth 279:154
6. Furedi-Milhofer H, Tunik L, Bloch R, Garti N (1994) Mol Cryst Liq Cryst 248:199
7. Gardner GI (1976) J Colloid Interface Sci 54:298
8. Brecevic Lj, Skrtic D, Garside J (1986) J Cryst Growth 74:399
9. Davis CW (1962) Ion association. Butterworths, London
10. Seddon KR (2004) Cryst Growth Des 4:1087
11. Desiraju GR (2004) Cryst Growth Des 4:1089
12. Bernstein J (2005) Cryst Growth Des 5:1661
13. Joseph S, Kamath PV (2006) J Electrochem Soc 153:D99
14. Golden TD, Shumsky MG, Zhou Y, VanderWerf RA, Leeuwen RAV, Switzer JA (1996) Chem Mater 8:2499
15. Joseph S, Kamath PV (2008) Solid State Sciences 10:1215
16. Xu S, Melendres CA, Park JH, Kamrath MA (1999) J Electrochem Soc 146:3315
17. Windhausen AB, Switzer JA (2008), Abstracts, 64th Southwest Regional Meeting of the American Chemical Society, Little Rock, AR, United States
18. Switzer JA (1987) Am Ceram Soc Bull 66:1521
19. Kajita T, Kogyo N-S (1995) Kenkyusho Kenkyu Hokoku 80:22
20. Kajita T (1989) Hyomen Kagaku 10:181
21. Joseph S, Kamath PV (2007) J Electrochem Soc 154:E102
22. Dinamani M, Kamath PV, Seshadri R (2003) Solid State Sci 5:805
23. Young RA (1993) The Rietveld Method. IUCr monographs on crystallography no. 5. Oxford University Press, New York
24. Ostwald W (1897) Z Phys Chem Stechiom Verwandtschaftsl 22:289